

Levee failure mechanisms during the extreme rainfall event: a case study in Southern Taiwan

Wen-Chao Huang · Meng-Chia Weng · Ray-Kuo Chen

Received: 23 April 2013 / Accepted: 21 September 2013 / Published online: 29 September 2013
© The Author(s) 2013. This article is published with open access at Springerlink.com

Abstract Extreme weather has recently caused many disasters worldwide. In August 8, 2009, Southern Taiwan suffered from serious floods during Typhoon Morakot. In this extreme rainfall event, the Chiuliao first levee in the Laonong River basin experienced catastrophic failure. Therefore, this study focuses on the levee failure mechanisms based on variations in levee water levels. Specifically, this study investigates four mechanisms based on limit state equilibrium. The first mechanism involves the slope stability under hydrostatic conditions at various water levels. The results of this analysis show that the levee cannot fail under this mechanism. The second mechanism involves the levee slope stability with steady-state seepage. Because the water levels are different on the protected and flood sides, the water recedes much faster on the flood side than the protected side. Based on this analysis, the levee slope might fail when the water level at the protected side is close to the top of levee and the water level at the flood side starts to recede. The third and fourth mechanisms involve the levee foundation failure in terms of sliding and overturning failure. The results of this study indicate that the levee foundation is more prone to sliding failure than overturning failure. Based on these results, this study shows that the levee failed when the water level at the protected side neared the top of levee while the water level at flood side started to recede. At this moment, the levee may fail because of both the slope failure with seepage and sliding failure of the levee foundation.

Keywords Breach · Levee · Extreme weather · Typhoon

1 Introduction

Because it is located in a subtropic area, Taiwan experiences severe disasters induced by typhoons during the summer season and has a mean precipitation from 2,500 mm/year up

W.-C. Huang · R.-K. Chen
Department of Civil Engineering, National Central University, Chungli, Taiwan

M.-C. Weng (✉)
Department of Civil and Environmental Engineering, National University of Kaohsiung,
Kaohsiung, Taiwan
e-mail: mcweng@nuk.edu.tw

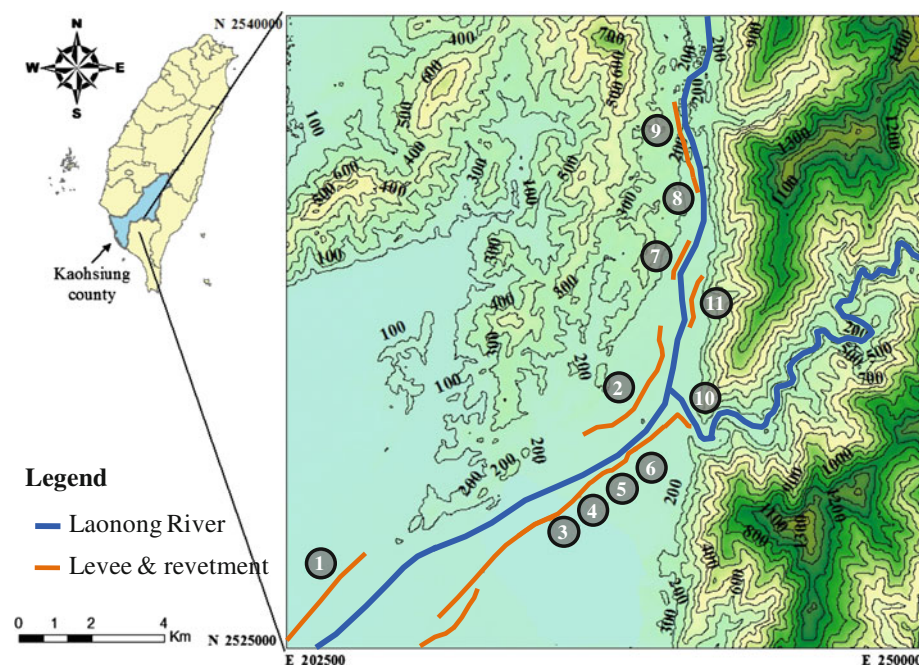


Fig. 1 Locations of levee breaches in the downstream area of the *Laonong River* after Typhoon Morakot. (Chiuliao first levee is in location No. 6, Liu et al. 2009)

to 3,000 mm/year in mountainous areas. The enormous rainfall that accompanies typhoons frequently causes floods. Recent extreme events, such as the 2001 Toraji Typhoon, the 2004 Mindulle Typhoon, the 2005 Haitang Typhoon, and the 2009 Morakot Typhoon, induced catastrophic damage. On August 8, 2009, Typhoon Morakot invaded Southern Taiwan and caused significant loss of life and property (Lin et al. 2011; Wu et al. 2011; Weng et al. 2011). Morakot was the most damaging typhoon in Taiwan in half a century. It sets a new rainfall record in the Laonong River basin, and the accumulative rainfall was up to 2,500 mm in 4 days, which represents the extreme rainfall event herein. Many levees and revetments along the Laonong River were damaged during this event, and the river basin suffered severe flood disasters. Figure 1 shows the locations of levee breaches and revetment failures in the downstream area of Laonong River (Liu et al. 2009). The levee system experienced catastrophic damage during the typhoon, causing intense land scour and flooding in villages along the river.

Among the levee breaches above, the most serious disaster occurred at the Chiuliao first levee, which is located in Kaoshu village in Pintung County (No. 6 in Fig. 1). This levee was built on the left river bank near the confluence of the Laonong River and its branch, the Chokuo River. This levee is a gravity-type earthen levee with a height of approximately 10 m. During Typhoon Morakot, approximately 4,000 m of the levee broke away, providing an opening for water to scour the protected side of the structure (Fig. 2). Approximately 0.5 km² of agricultural area behind the levee was eroded and more than 20 houses were destroyed (Figs. 2, 3) (Li et al. 2009; Liu et al. 2009; Chang 2012). This event drew significant public attention to the issue of levee safety.

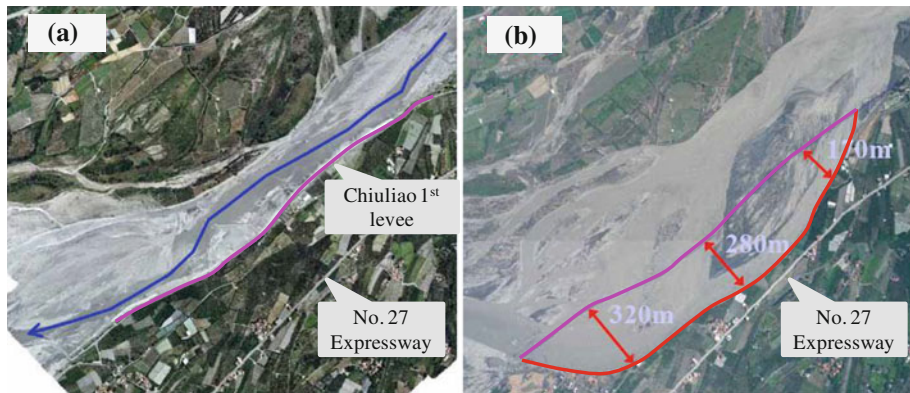


Fig. 2 Aerial photographs of the Chiuliao first levee breach before and after Typhoon Morakot. The breach length is approximately 4,000 m, and the maximum side erosion is approximately 320 m (Chang 2012). **a** Before Typhoon Morakot; **b** after Typhoon Morakot

The failure mechanisms of a levee system during a flood include several factors, they are as follows: (1) overtopping, (2) scouring of the foundation, (3) seepage/piping of levee body, and (4) sliding of the foundation (Ojha et al. 2001; Serre et al. 2008; Sills et al. 2008). These failure conditions are influenced by the levee's geometrical configuration, hydraulic conditions (e.g., river level and seepage), and material properties (e.g., grading, cohesion, compaction, and water salinity). Among these failure mechanisms, overtopping, which indicates the flood waters exceed the design capacity of the levee and flow over the structure, is a common failure mechanism. During Hurricane Katrina, the levee system surrounding New Orleans experienced catastrophic overtopping, bringing approximately 80 % of the city under water. Many researchers have studied the stability of levees under overtopping flow (ASCE Hurricane Katrina External Review Panel 2007; Briaud et al. 2008; Ubilla et al. 2008; Seed et al. 2008a, b; Storesund et al. 2010; Song et al. 2011; Xu et al. 2012). However, in the case of Chiuliao first levee, overtopping was not the main failure mechanism. According to the field investigation and the report of eyewitness after Typhoon Morakot (Li et al. 2009; Chang 2012), no flood evidences on the protected side of the levee were found, such as flow traces or inundation in the lower area. Therefore, other mechanisms must have caused this levee breach (Table 1).

This study explores the main mechanism for flooding disasters, which result in levee breaching and foundation failure. We first determined the geotechnical properties of the levee and the site, and then applied the limit equilibrium method to analyze the levee behavior and foundation stability when heavy rain occurred. This study attempts to identify the reasons for potential damage and describes the levee breaching process.

2 Methodology

2.1 Evaluation of in situ geotechnical parameters

We collected soil boring information near the study site to perform the relevant analyses in this study. Based on the lack of soil boring information for small-scale levees, we had to collect the required information from a nearby Da-Jin Bridge construction site (Directorate

Fig. 3 Field investigation after Typhoon Morakot (Li et al. 2009). **a** Side erosion at the river bank; **b** collapsed building



(a)



(b)

Table 1 Failure conditions of levees and revetments on the Laonong River during Typhoon Morakot (Liu et al. 2009)

No.	Location	Failure condition
1	Gueishan levee	About 200 m levee breaches due to flood
2	Hsinliao revetment	About 920 m revetment breaches due to flood
3	Tsailiao revetment	Total collapse due to flood
4	Chiuliao second levee	About 270 m levee breaches due to flood
5	Chiuliao first revetment	Total collapse due to flood
6	Chiuliao first levee	Total collapse due to flood
7	Erpo revetment	About 750 m revetment breaches due to flood
8	Hsinhsing levee	Total collapse due to flood
9	Hsinhsing revetment	About 1,090 m revetment breaches due to flood
10	Dachin third revetment	Total collapse due to flood
11	Dachin first revetment	About 1,070 m revetment breaches due to flood

General of Highways MOTC 2004). This information includes the area geologic map, generalized soil profiles, and a few laboratory and in situ test results. The geologic information indicates that the bedrock consists of mostly shale and slate rocks, with occasional sand rock. We performed six soil borings near the study site. Soil boring site numbers B-1 and B-6 were made close to the bridge abutment, and sites B-2–B-5 were made at the elevation of riverbed. The soil borings depth was 25 m. Figure 4a shows the relative location of collected soil borings and Chiuliao first Levee, and Fig. 4b shows the generalized soil profile variation with respect to elevation. Figure 4b shows that the top 20 m of the in situ site condition is mostly gravel layer, with bedrock located at an elevation of approximately EL. 125 m.

The soil borings provided information about the standard penetration test (SPT-N) values, physical properties, and engineering properties of the soil. These reports summarized the physical properties of soils, including basic classification, natural water content, unit weight, void ratio, Atterberg limits, specific gravity, and engineering properties such as friction angles and cohesion values. The unit weight ranged from 19 to 22 kN/m³, and the SPT-N values are close to a maximum of 50 blows. The friction angles listed in the report ranged from 30° to 35°. However, based on the generalized soil profile, the soils are mostly gravel and the friction angles from laboratory testing seem to be too conservative. Therefore, we used the empirical equations of Schmertmann (1975) and Hatanaka and Uchida (1996) to relate SPT-N values with friction angles, and the evaluated friction angles ranged from 37° to 45°.

$$\tan \varphi \approx \left[\frac{N}{\left(12.2 + 20.3 \frac{\sigma'_{v0}}{p_a} \right)} \right]^{0.34} \quad (\text{Schmertmann 1975}) \quad (1)$$

$$\varphi = (20N_1)^{0.5} + 20 \quad (\text{Hatanaka and Uchida 1996}) \quad (2)$$

where ϕ is the friction angle, N is the in situ SPT-N value, σ'_{v0} is the effective vertical stress, p_a is the reference stress (equal to atmospheric pressure), and N_1 is the SPT-N value modified based on effective stress.

Figure 5 shows the variation of friction angles based on laboratory tests and empirical equations. One can observe that most of the friction angles derived based on empirical equations are close or equal to 45°, and this is due to the fact that the empirical equations are more suitable for sandy soils. Because there are limited empirical equations to evaluate the friction angles of gravelly material, the results of estimated friction angles are further compared to friction angles derived in the laboratory, as shown in Fig. 5. Based on the friction angle information in Fig. 5, we varied the analyzed friction angles 35° and 45° to capture the sensitivity of friction angles in the failure mechanisms considered in this study.

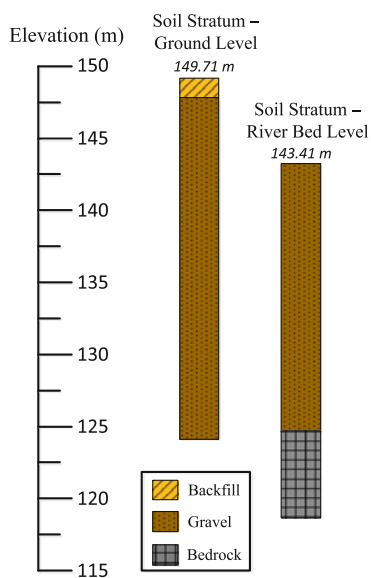
In addition to the in situ soil properties, we collected the design profiles of the levee before and after Typhoon Morakot to perform the relevant analysis of levee stability (Fig. 6). Before Typhoon Morakot, the levee foundation was constructed directly on the in situ soil layers, with a 1.5-m layer of backfill and a layer of rockfill to stabilize the flood side of the levee.

2.2 Analysis method

This study investigates the influence of extreme rainfall on the stability of Chiuliao first levee through several scenarios. First, with the increase in accumulated rainfall along the river, the water level on the flood side and protected side rises to a certain height (but not necessarily the same height on each side). When the flow rate increases to a certain



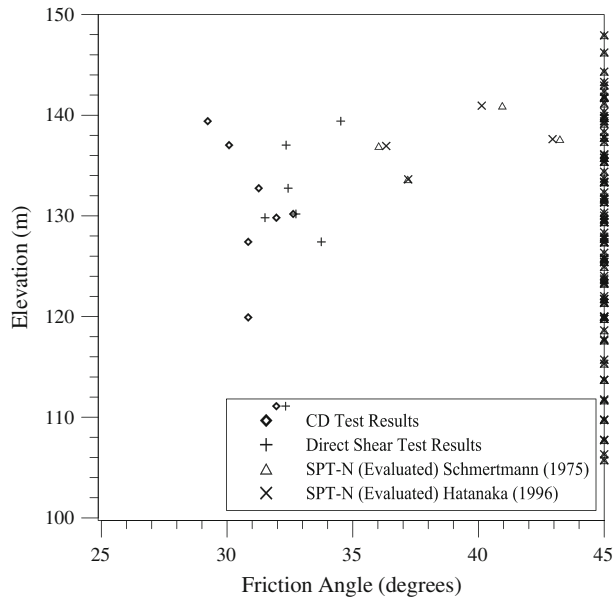
(a)



(b)

Fig. 4 Relative locations of soil borings and its soil profiles. **a** Locations of the Chiuliao first levee and soil borings; **b** generalized soil profiles close to the Chiuliao first levee

Fig. 5 Friction angles by laboratory testing results and empirical equations



threshold and the flow section decreases close to the downstream, the flow velocity could also increase (Chanson 2004). This increase induces scouring of the riverbed and the backfill of the levee foundation. Because the compacted backfill on the protected side is prone to erosion, the levee failure state could occur under high potential when the water level reaches the top of the levee.

A levee as a whole system can fail like a regular slope at various water levels and scouring depth conditions. Thus, the analyses in this study varied the water-level height and the scouring depth to check the safety of the slope. Because the chosen water-level height in the protected and flood side can be different, this study uses seepage-induced pore-water pressure to examine the stability of the levee from a slope stability viewpoint. According to the previous research projects, this study defines the water level corresponding to different return period of rainfall in Chiuliao first Levee cross section. Even for a 200-year flood return period, the water level only rises approximately two-thirds of the designed levee height. However, the analyzed water levels were chosen from the top of the levee and below to analyze extreme rainfall events.

Conversely, the foundation of the levee is a key factor influencing the stability of the levee. As Fig. 6a shows, the original design of the levee foundation plays an important role in stabilizing the levee system. Once the foundation is destabilized because of external factors, such as scouring or water-level variations, the whole levee may become unsafe. For these reasons, we also analyzed the levee foundation at different scouring depths and water levels on the protected and flood sides. Scouring effect was considered in the slope stability analysis without seepage. In slope stability and retaining wall stability analyses coupled with seepage, due to the fact that the stability relies highly on the existence of passive resistance (water or passive forces), once the backfill was carried away, the loss of passive resistance could cause immediate failure of the retaining wall or slope stability with seepage. In this study, only a few cases of slope stability and retaining wall stability with seepage were considered with scouring under higher water levels, which correspond to a more critical state of the levee. This study does not consider the scouring effect for the

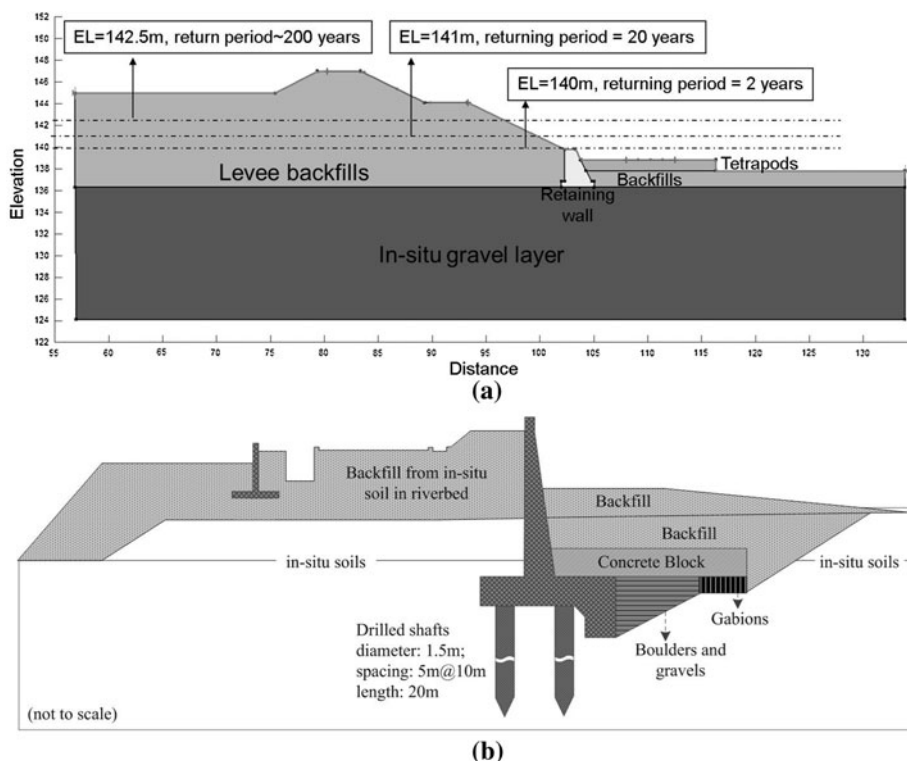


Fig. 6 Illustration of the levee profile of the Chiuliao first levee. **a** Levee profile before Typhoon Morakot; **b** design levee profile after Typhoon Morakot

levee foundation because the passive forces that provide additional resistance forces decrease when scouring occurs. This causes the backfill in front of the levee foundation on the flood side to disappear. The levee automatically fails under this circumstance. In summary, the failure mechanisms analyzed in this study include (1) slope stability analysis (considering seepage flow and water-level variation) and (2) levee foundation stability analysis (including typical retaining wall analyses—sliding and overturning failure under various water-level conditions). This study does not consider bearing capacity failure because the in situ friction angle of the gravel is so high that the levee foundation is not prone to bearing capacity failure. Figure 7 shows the relationships between the failure-triggered factors and the failure mechanisms.

We used the assumptions by Spencer under SLOPE/W software from Geostudio 2007 for the slope stability analysis. This slope failure mode considers a circular failure plane that moves toward the flood side. Spencer's method of the slope stability analysis also considers the vertical and horizontal forces between the slices, in addition to the force and moment equilibrium. Therefore, safety factors reported in this study are all based on Spencer's method. In addition, because of the variation of water levels in the analysis, we performed the seepage analysis using SEEP/W and combined the seepage analysis results with the slope stability analysis to determine the effects of seepage flow.

The variables used in this study include two categories. The first category is the strength parameter, or the in situ soil friction angle ψ , and the second category includes the water level

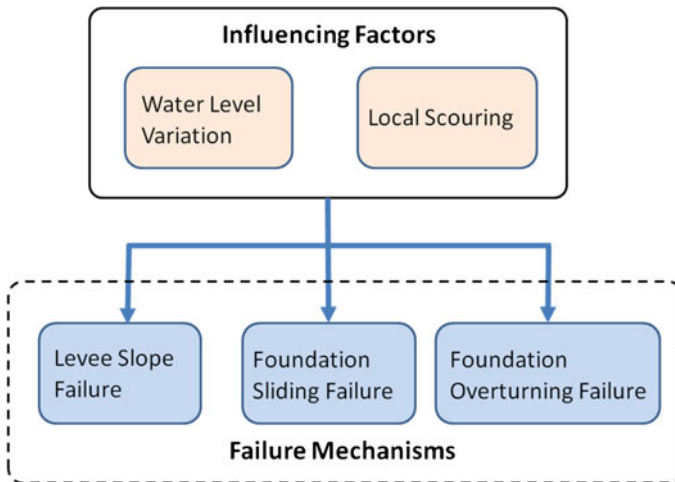


Fig. 7 Failure mechanisms considered in this study

and scouring depth of the riverbed on the protected side. The water level is defined as the water height on the flood side from the in situ ground surface. Because there is difference between protected flood sides of the water level, the difference is termed as water-level difference. The scouring depth is defined as the height from the backfill surface on the flood side. Figure 8 shows these parameters to enable better comprehension of the analyzed cases.

As mentioned previously, we also analyzed the levee foundation (as a retaining wall) based on sliding and overturning failure mechanisms. Figure 9 shows the dimensions of the levee foundation. Several external forces act on the foundations. On the left side of the foundation, there is active earth pressure and water pressure. On the right side of the foundation, there is passive earth pressure and water pressure. On the bottom of the foundation, there is uplift force caused by pore-water pressure. To determine the pore-water pressure distribution when the water level heights at both sides of the foundation are different (thus inducing seepage), we used SEEP/W to obtain the pore-water pressure distribution under the foundation. The foundation was considered to be sliding when the horizontal driving forces exceeded the horizontal resistance forces. Overturning of the foundation was considered through the resistance moment against the driving moments with respect to the toe of the levee foundation. The weight of the foundation was calculated based on the design cross section of the levee system.

3 Analysis of results and discussion

3.1 Slope stability analysis

In terms of the slope stability analysis, the water levels varied in two ways. The first situation is when the water levels are the same on both sides of the levee, and the second situation corresponds to the case that the water levels on both sides are different. For these water-level situations, we varied the friction angles of the in situ soils and the scouring depths to obtain the slope stability factor. When the water levels on both sides of the levee are the same, the seepage stops because the water has reached a hydrostatic condition.

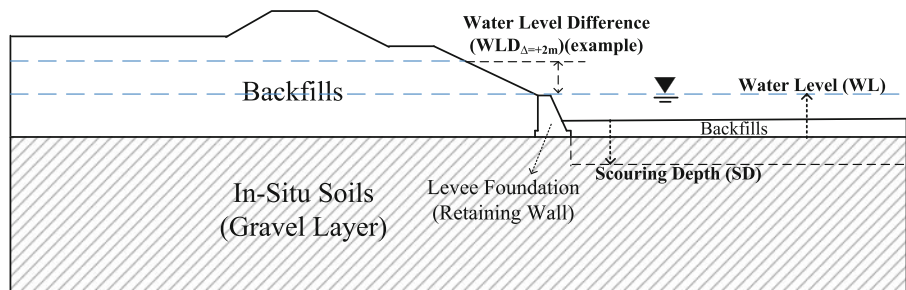


Fig. 8 Illustration of the levee stability analysis parameters: water level (WL), water-level difference (WLD), and scouring depth (SD)

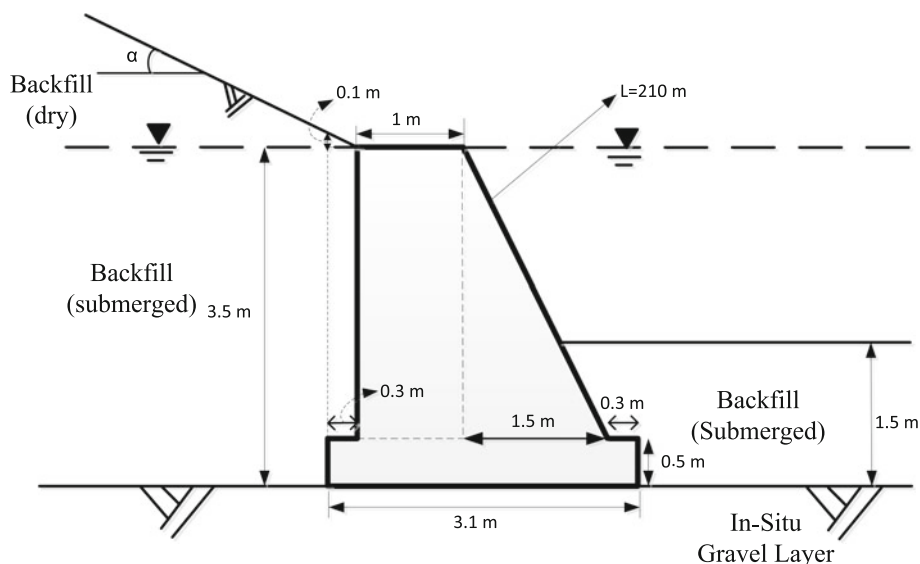
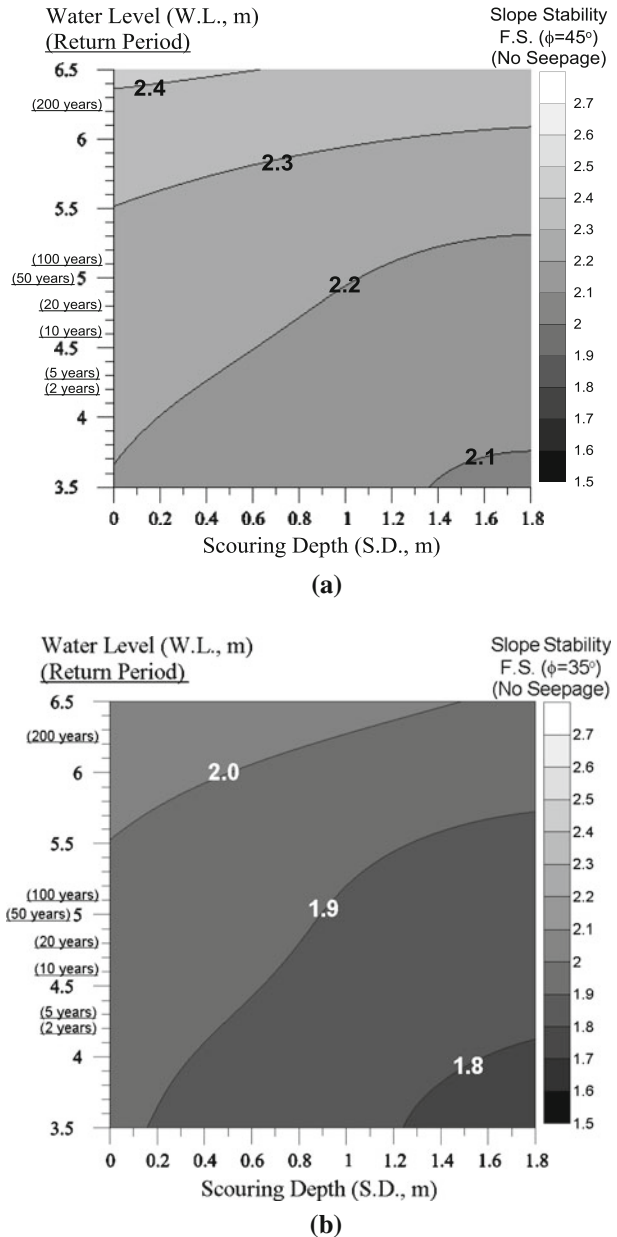


Fig. 9 Schematic illustration of the levee foundation cross section

When the water levels on the two sides of the levees are different, we assumed steady-state seepage because of a difference in hydraulic heads, which indicated that the water level in the protected side is higher than that in the river side. Along with varying these parameters, we also assumed that the tripod blocks were washed away under extreme weather conditions. In terms of scouring for the above two situations, we have assumed different scouring depths under no seepage case. For cases with seepage, we considered scouring only when the water level at protected side was at top of levee.

Figure 10 shows the variations in safety factor at different scouring depths and water levels. In Fig. 10, the water level was also expressed in terms of the flood returning period with friction angle of 45° and 35° . The analysis results show that as the scouring depth increases, the safety factor decreases, and as the water level increases, the safety factor also increases. This increasing safety factor with increasing water level is the result of increasing hydraulic pressure after the levee surface. Figure 10 also shows that the safety factors of all the analyzed cases are larger than 2 for both 45° and 35° , meaning that the

Fig. 10 Influence of scouring depth (SD) and water level (WL) on the stability of levee.
a $\phi = 45^\circ$; **b** $\phi = 35^\circ$



levee failure mechanism by slope failure with the same water level is less possible during an extreme weather event.

This study also considers the steady-state seepage with various water levels at two sides of the levees through the slope stability analysis (Fig. 11). This figure shows that the water level at the protected side is defined as h_1 and water-level difference is defined as protected side water level minus flood side water level. The flood water was clogged on the protected side such that the water only seeps from the protected side toward the flood side under the

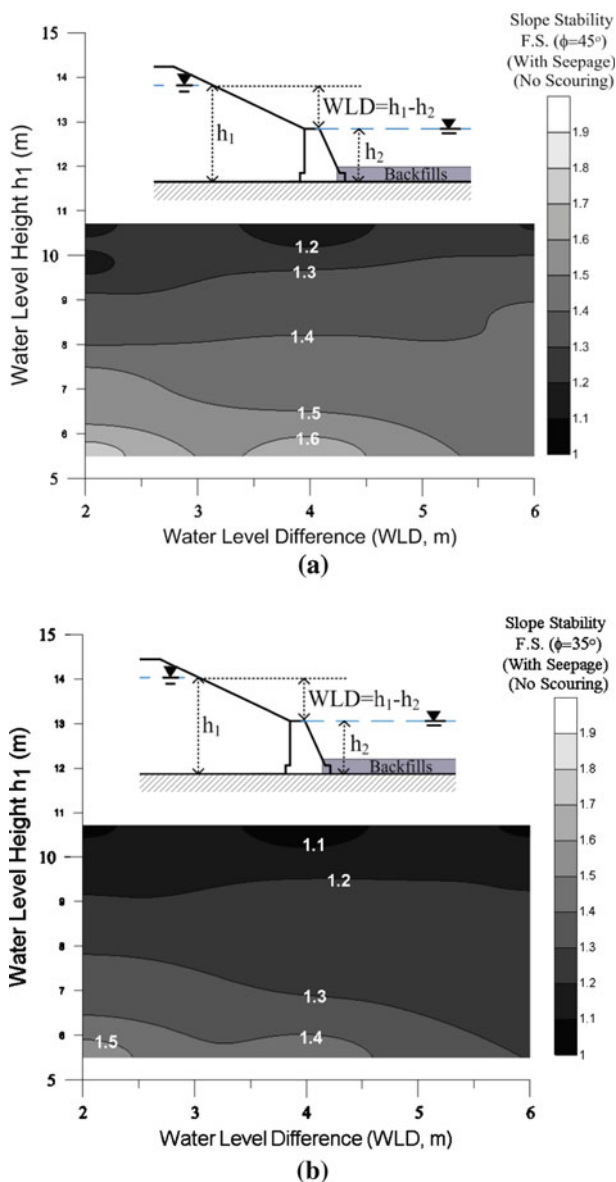


Fig. 11 Influence of water-level height on the stability of levee (with safety factor calculated based on the slope stability coupled with seepage effect). **a** $\phi = 45^\circ$; **b** $\phi = 35^\circ$

levee foundation. Therefore, the water-level difference is always positive in this study. In addition, the results shown in Fig. 11 do not consider the scouring depth. Based on the slope stability viewpoint with steady-state seepage, the safety factor is more sensitive to variations in the protected side water level. For example, in Fig. 11a, when h_1 varies from 9 to 10.7 m, it causes a variation of safety factors from 1.1 to 1.3. For the same protected side water level, the change of water-level difference does not cause too much variation in

the corresponding safety factor. In addition, the sensitivity of the water-level difference toward the safety factor depends on the protected side water level. Figure 11a shows that when the water-level difference is a constant, the change of water level on the protected side caused a more sensitive response on the safety factor, especially when the water level is high. This indicates that a high water level on the protected side is itself a deteriorating factor that reduces the overall safety of the levee. When the protected side water level is close to the top of levee, the slope stability safety factor is in a critical range such that a small amount of water-level difference might cause levee slope failure. The input friction angle for the results shown in Fig. 11 is 45° , which is close to the upper bound of the analyzed friction angle. Figure 11b also showed the analyzed results under 35° of friction angle, which correspond to a lower bound value. Figure 11a, b can be employed to understand the possible outcomes under a lower and higher friction angles. From Fig. 11, it was found that the influence caused by a difference of 10° was not too significant in terms of the slope stability analysis.

In some extreme cases of water level, the safety factors might be close to 1. Therefore, a clogging-induced rise in the water level on the protected side might decrease the safety of the levee from a slope stability viewpoint. Scouring effect was considered in the slope stability analysis coupled with seepage; however, it was only analyzed when the water level at the protected side reached top of levee. This is due to the fact that when the water level in the protected side is close to the top of levee, it was found that the safety factor is more critical when scouring was not taken into account, as shown in Fig. 11. When scouring depth was 0.5 m (i.e., about one-third of the backfill thickness), the safety factor was 1.02, 0.997, and 0.981 under a water-level difference of 2, 4, and 6 m (the above factors of safety were derived based on a 45° friction angle). It is therefore expected that further scouring can cause the slope to fail with seepage condition. The analyzed results also indicate that scouring coupled with seepage condition deteriorates the slope stability factor of safety even further, especially when the water at the flood side just receded from the top of levee; (this critical situation corresponds to a water-level difference of 2 m).

3.2 Levee foundation failure analysis

The second failure mechanism considered in this study is the levee foundation stability. Levee foundation stability involves sliding, overturning, and bearing capacity failure. As mentioned previously, because the in situ soil contains mostly gravel material, the friction angle might be large enough to prevent bearing capacity failure. With just one case with friction angle of 35° , the factor of safety against bearing capacity failure of levee foundation is approximately 20. This indicates that the levee foundation is not subject to bearing capacity failure. Therefore, the analyses in this study focus on the sliding and overturning failure of the levee foundation. Based on the levee design profile, it was found that a layer of backfill was in front of the retaining wall. Tripod rocks are above the compacted backfill. In this part of the analysis, it was assumed that the tripod rock was carried away by the flood; therefore, only backfill layer is present in front of the retaining wall. The reason to keep the backfill in this part of the analysis is that during preliminary retaining wall analysis, it was found that the stability of the retaining wall relies highly on the existence of the backfill; once the backfill was eroded partially or fully, the only passive resistance force that keeps the retaining wall stable decreases or disappears. Hence, possible failure due to the instability of retaining wall occurred.

To understand the response of levee foundation to variations in the water levels on the protected and flood sides, we varied the water levels between the top of the levee and the

top of the levee foundation. When the water levels on both sides of the levee foundation were different, we performed the seepage analyses to determine the pore-water pressure distribution under the levee foundation. We assumed that the water level is always higher or equal to the water level on the protected side than the flood side. We also analyzed the levee foundation stability. The forces acting on the levee foundation include (1) the active earth pressure from the protected side of levee, (2) the passive earth pressure from the flood side of the levee (although this is backfill material, we assumed that passive earth pressure is still present), (3) water pressure from both sides of the levee foundation, where the water pressure depends on the corresponding water level, and (4) uplift force from the bottom of the levee foundation, which is induced by the pore-water pressure acting on the impervious levee foundation bottom boundary. Figure 9 shows the detailed geometry of the levee foundation.

The results in Fig. 12 show the levee foundation stability against sliding with friction angles of 35° and 45° . These figures show that an increase in the water level on both the flood side and protected side decreases the stability against sliding. The increase in the water level on the flood side (h_2) is not as sensitive to the variation of protected side water level (h_1). When the flood side water level nears the top of the levee (i.e., reaches 9–10.7 m), the safety factor against sliding ranges from 1.2 to 1.4, but is not sensitive to a variation in water level on the protected side. The safety factor changes most rapidly in the following two conditions:

The safety factor changes most rapidly in the following two conditions. The first condition (Condition 1) indicates that levee is in a stable state when the protected side water level is between 3.5 and 4.5 m with flood side water level between 3.5 and 5 m. The second condition (Condition 2) represents a critical state of the levee. The critical state occurs at 6–10.5 m of the protected side water level and 1.5–6.5 m of the flood side water level.

The safety factors against sliding in Condition (1) are greater than 1.5, showing that the levee foundation is still in a stable state despite rapid variations in the safety factor. This is also reasonable because the water levels on both sides of the levee are in the lower range of the expected water level. Therefore, no failure is expected for this water-level range. In Condition (2), which shows a relatively high water levels at both sides of the levee, the corresponding maximum safety factor is about 1.3, which is an acceptable value against sliding. However, as the water level on the flood side starts to recede, the safety factor starts to decrease to a value of approximately 1–1.1 when the water level on the flood side changes 4–5 m. This is a critical failure state for the levee foundation, which may undergo sliding failure.

Figure 13 shows the variation of water levels and the corresponding variations of safety factor against overturning failure. A similar trend here is that the safety factor against overturning is more sensitive to water-level variations on the protected side than the flood side. Similarly, when the flood side water level is close to the top of levee, the corresponding safety factor is always greater than 1.3. The overturning failure considered in this study is when the levee foundation overturns toward the flood side. Therefore, when the flood side water level is high, it provides an additional stabilization moment against overturning failure. Another extreme situation is when the protected side water level is close to the top of levee. When the flood side water level has receded, the corresponding safety factor against overturning reaches 1.1–1.2. Then, the water level on the protected side ranges from 6 to 10.7 m and the flood side water level ranges from 3 to 5 m; the overturning safety factor is not acceptable, with a value always smaller than 1.2.

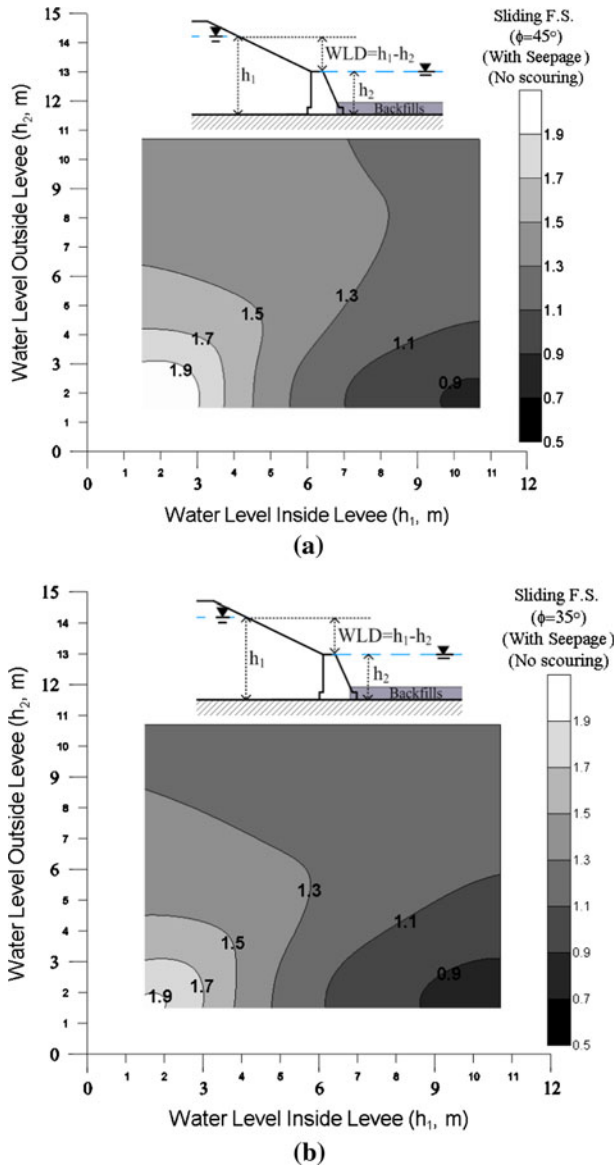


Fig. 12 Influence of water level on sliding safety factors of the levee foundation with different friction angles. **a** $\phi = 45^\circ$; **b** $\phi = 35^\circ$

A comparison of the levee foundation failure modes between sliding and overturning shows that the analyzed levee foundation is more prone to sliding failure than overturning failure. Analyzing the same water-level scenario for both sliding and overturning failure shows that the sliding safety factor is always smaller than the overturning safety factor. Under extreme water-level conditions, when the protected side water level is close to the top of the levee and the flood side water level recedes to a relatively low level, the corresponding safety factor for sliding is even smaller than the safety factor for overturning

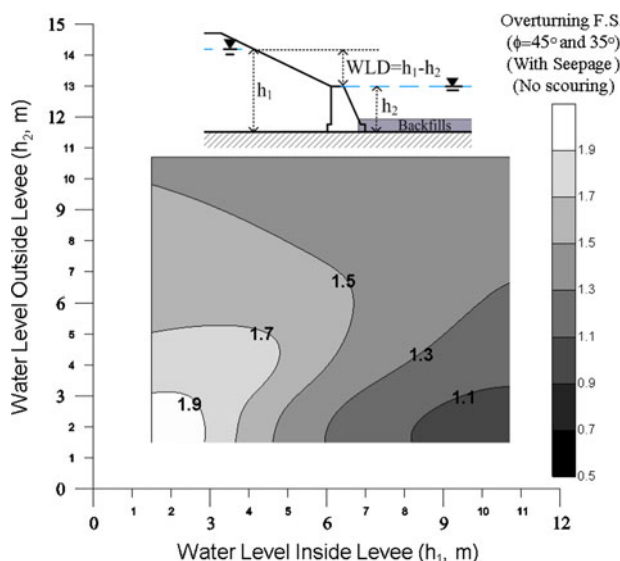


Fig. 13 Influence of water level on overturning safety factors of the levee foundation with different friction angles

failure. Based on this case study, we concluded that sliding failure is more of a concern than the overturning of the levee foundation. The possibility of foundation sliding failure can also lead to side erosion of the river bank. Figure 3a shows a similar phenomenon. Scouring was also considered for the retaining wall stability under full water level at protected side of levee and 2, 4 and 6 m water-level difference. The scouring depths were 0.5 and 1.5 m. In addition, since the critical safety factor among most of the retaining wall safety factors is the sliding failure safety factor, the following safety factors are reported as the sliding safety factors. The corresponding safety factors under a scouring depth of 0.5 m are 1.12, 1.04, and 0.92 with 2, 4, and 6 m water-level difference. The corresponding safety factors under a scouring depth of 1.5 m are 1.04, 0.95, and 0.81 with 2, 4, and 6 m water-level difference. It was found from the results that when scouring was coupled in the analysis, the safety factor became less than 1 easily; it was therefore concluded that scouring coupled with seepage is indeed a deteriorating factor in influencing the stability of the levee foundation.

4 Failure mechanism of the Chiuliao first levee

This study investigates the failure mechanisms based on the following conditions:

1. Mechanism 1: Slope stability under hydrostatic condition.
2. Mechanism 2: Seepage-induced slope instability with scouring depth 0.5 m.
3. Mechanism 3: Levee foundation failure—sliding failure with scouring depth 0.5 m.
4. Mechanism 4: Levee foundation failure—overturning failure with scouring depth 0.5 m.

Table 2 shows a summary of the safety factors corresponding to various water levels for these mechanisms. For slope stability under hydraulic static conditions, the acceptable

Table 2 Safety factors under different failure mechanisms and water-level conditions ($\phi = 45^\circ$, $\phi = 35^\circ$)

Water level (protected– flood side)	Slope stability (no seepage) (accepted FS = 1.5)	Slope stability (seepage) (accepted FS = 1.3)	Retaining wall sliding failure (accepted FS = 1.3)	Retaining wall overturning failure (accepted FS = 1.3)*
8.5–8.5 (SD = 1.5)	2.42, 1.96	–	–	–
5–5 (SD = 1.5)	2.08, 1.71	–	–	–
3.5–3.5 (SD = 1.5)	1.94, 1.62	–	–	–
10.7–8.7 (WLD = 2)	–	1.19, 1.04	1.26, 1.20	1.33
10.7–6.7 (WLD = 4)	–	1.13, 1.05	1.19, 1.12	1.27
10.7–4.7 (WLD = 6)	–	1.19, 1.09	1.09, 1.01	1.19
9.5–7.5 (WLD = 2)	–	1.18, 1.11	1.26, 1.20	1.35
9.5–5.5 (WLD = 4)	–	1.23, 1.12	1.18, 1.10	1.28
9.5–3.5 (WLD = 6)	–	1.33, 1.19	1.06, 0.96	1.17
8.5–6.5 (WLD = 2)	–	1.33, 1.22	1.30, 1.22	1.41
8.5–4.5 (WLD = 4)	–	1.39, 1.25	1.20, 1.11	1.33
8.5–2.5 (WLD = 6)	–	1.42, 1.25	<1.0, < 1.0	~1.0

* The overturning stability safety factor was not influenced by the change of in situ friction angle

safety factor was set as 1.5 for evaluating slope stability. For slope stability under steady-state seepage, the acceptable safety factor was set as 1.3 for extreme rainfall events. The same value was chosen for levee foundation stability under both sliding and overturning failure.

For the slope stability case without seepage, the safety factors of all the analyzed cases were above 1.5, indicating that the levee is stable under Mechanism 1. For Mechanism 2, we analyzed the slope stability of levee with steady-state seepage. Table 2 shows that the safety factor falls below 1.3 mostly when the water level on the protected side is close to the top of the levee. When the water level on the flood side falls below 8.7 m, the safety factor becomes critical and the levee is prone to failure. The levee foundation stability against sliding also shows similar behavior for Mechanism 3. The safety factor against levee foundation sliding becomes critical when the water level on the protected side is close to the top of the levee. When the water level on the flood side decreases, the safety factor decreases accordingly. This may be because of the static water pressure acting on the levee surface from the flood side. When the water level on the flood side decreases, the water pressure acting on the levee flood side also decreases, hence reducing the force against sliding. Although other water levels produce a lower safety factor, all of these water levels require a certain amount of water-level reduction in the protected and flood

sides of the levee. Before a much lower water level occurs, the safety factor reaches a critical state and failure is imminent. Mechanism 4 exhibits a trend similar to the sliding failure mechanism. The only difference is that overturning failure could only occur when the water level on the protected side is close to the top of the levee when the flood side water level is 4.7 m. This flood side water level is much lower than those in Mechanisms 2 and 3. In addition, under the same water-level conditions, the safety factor for overturning failure is consistently higher than that for sliding failure. Therefore, overturning failure is less possible than sliding failure for the levee analyzed in this study. The analysis results shown in Table 2 were obtained with in situ friction angle of 45° and 35° . The results for retaining wall and slope with seepage did not take into consideration the scouring effect in the results reported in Table 2. The summarized results showed a minor influence on the variations of friction angles. However, as the safety factor from a denser material showed critical state already, with a looser material, the safety factor could become less than 1, therefore resulting in an instable state from different failure mechanisms.

After analyzing all the possible water-level cases under the levee foundation failure criterion, we proposed a possible scenario of how the levee foundation failure occurs (Fig. 14). First, when the water rises because of rapid and long-duration rainfall (such as that during Typhoon Morakot), the water rises on both sides of the levee until it reaches the top of the levee (or close to the 200-year flood return period). When the water starts to recede on the protected side, the water on the flood side can recede such that the water level decreases. The imbalance of water levels on both sides of the levee causes seepage flow and increases the uplift force applied from the bottom of the levee foundation. Figure 14 shows a scenario in which the water level on the protected side is close to the top of the levee, whereas the water level on the flood side of the levee starts to recede. When the water-level difference reaches approximately 4 m, the safety factor against sliding becomes smaller than 1.2, whereas the safety factor against overturning is 1.27. These safety factors are all smaller than the values before the water level on the flood side decreased. When the water levels change to the second stage (Fig. 14), the levee foundation reaches a critical state with possible sliding failure. As the water level continues to decrease, the levee foundation might move laterally and overturn counterclockwise.

As shown in Fig. 14, the failure of the Chiuliao first levee might involve two major mechanisms. The first mechanism is the slope failure under steady-state seepage. The second mechanism is the levee foundation sliding failure, which causes possible sequence for the levee to reach failure state. As the water level increases on both sides of the levee,

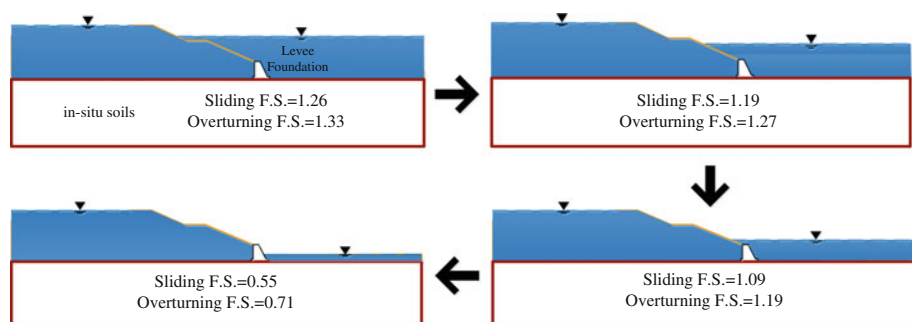


Fig. 14 Analyzed safety factors (the first safety factor represents the sliding safety factor and the second represents the overturning safety factor) under various water-level situations with in situ $\phi = 45^\circ$ (only tripod rocks were assumed to be carried away)

the safety factor remains acceptable until the water levels reach the top of the levee. If the water mass remains on the protected side while the water on the flood side recedes, both the levee slope and the levee foundation may fail because of the water-level difference. Although a high water level is one of the possible mechanisms triggering failure, other mechanisms might be more likely to be triggered under more critical water-level situations. It is also to be emphasized that the results reported in the figures or table do not take into consideration the scouring depth, due to the fact that once scouring was analyzed with the corresponding failure mechanism, all of the safety factors become even smaller. Hence, all of the safety factors might become smaller when scouring occurred in the field.

Figure 6b shows the design cross section of Chiuliao first levee after Typhoon Morakot. Two rows of piles were added to the bottom of the cantilever levee foundation, and gabions and rocks were also added to the flood side of the levee to provide additional weight for stabilization. The application of rows of piles under the levee foundation might be able to resolve the possible failure mechanisms discussed in this study. Although further analysis regarding the new cross section has not been performed, these rows of piles can provide additional forces against sliding and overturning. The application of piles can also provide tension forces when a high water level causes a high pore-water pressure, which in turn induces uplift force that deteriorates the levee foundation. The application of piles can also force the potential slope failure surface to go down, increasing the safety factor against slope instability.

5 Summary and conclusion

The Chiuliao first levee experienced catastrophic failure because of an extreme rainfall event during Typhoon Morakot. Because the amount of rainfall almost hit a world record, this study focuses on levee failure mechanisms based on the variations in water levels on both sides of the levee. This study analyzes four mechanisms. First, we considered the slope stability under hydrostatic conditions and various water levels. The results of this analysis show that the levee cannot fail under this mechanism. The corresponding safety factor exceeds 1.9. The second mechanism involves the levee slope stability with steady-state seepage. Because the water levels are different on the protected and flood sides of the levee, the water recedes much faster on the flood side than the protected side. Based on these analysis results, the levee slope might fail when the water level at protected side is close to the top of levee while the water level at the flood side started to recede. The second mechanism is therefore a possible failure mechanism for the failure of the Chiuliao first levee during Typhoon Morakot. The third and fourth mechanisms involve the sliding and overturning failure of the levee foundation—retaining wall. Variations in the water level caused changes in the safety factor against retaining wall sliding and overturning failure. However, the studied levee was more sensitive to changes in the safety factor of sliding failure than to overturning failure. These results indicate that the levee foundation in this study is more prone to sliding failure than overturning failure. The levee foundation reached a critical state when the water level on the protected side is close to the top of the levee and the water level on the flood side of the levee starts to recede. This is just like the water-level situation that caused slope failure in the second failure mechanism. Under these conditions, the levee could experience slope failure because of seepage and sliding failure of the levee foundation.

An examination of the design cross section of the levee after Typhoon Morakot shows that the most significant feature of the new design is the addition of rows of piles. These

rows of piles in the levee design can develop stabilizing forces. This new levee design and the analyzed failure mechanisms can resolve a specific failure mechanism discussed in this study. Typical levee analysis involves the slope stability analysis to determine the stability under various conditions. However, extreme rainfall events seem to have a much shorter return period, and any possible failure mechanisms must be considered thoroughly under extreme conditions.

Acknowledgments The research is supported by the National Science Council of Taiwan, Grant No. NSC101-2218-E-002-001. The authors also thank Directorate General of Highways and Water Resources Agency of Taiwan for providing associated information.

Open Access This article is distributed under the terms of the Creative Commons Attribution License which permits any use, distribution, and reproduction in any medium, provided the original author(s) and the source are credited.

References

- ASCE Hurricane Katrina External Review Panel (2007) The New Orleans hurricane protection system: what went wrong and why. American Society of Civil Engineers, Reston
- Briaud J, Chen H, Govindasamy A, Storesund R (2008) Levee erosion by overtopping in New Orleans during the Katrina Hurricane. *J Geotech Geoenviron Eng* 134:618–632
- Chang LP (2012) The disaster investigation and improvement measures of hydraulic facilities after Typhoon Morakot. In: Proceedings of the conference of risk assessment for geotechnical facilities under extreme events. Taipei, Taiwan
- Chanson H (2004) The hydraulics of open channel flow: an introduction. Butterworth-Heinemann, Oxford
- Directorate General of Highways, MOTC (2004) Report of geological investigation at Da-Jin Bridge, Expressway No. 27. Taipei, Taiwan
- Hatanaka M, Uchida A (1996) Empirical correlation between penetration resistance and effective friction of sandy soil. *Soils Found* 36(4):1–9
- Li WS, Yeh KC, Lin CC, Shieh CL, Wen JC, Yeh YL, Hsieh LS, Chen LQ, Li HC, Wang YW (2009) Disaster survey and analysis of Morakot Typhoon. Research Report of National Science Council, Taiwan
- Lin CW, Chang WS, Liu SH, Tsai TT, Lee SP, Tsang YC, Shieh CL, Tseng CM (2011) Landslides triggered by the 7 August 2009 Typhoon Morakot in southern Taiwan. *Eng Geol* 123:3–12
- Liu CB, Tsai WH, Heish KJ, Lin CH, Chang DC (2009) Survey and improvement measures on Southern Taiwan hydraulic facilities after 88 Flood. *Sino Geotech* 122:95–104
- Ojha C, Singh V, Adrian D (2001) Influence of porosity on piping models of levee failure. *J Geotech Geoenviron Eng* 127(12):1071–1074
- Schmertmann JH (1975) Measurement of in situ shear strength, keynote lecture. In: Proceedings of the conference on in situ measurement of soil properties, vol II, pp 1–4
- Seed RB, Bea RG, Abdelmalak RI, Athanasopoulos-Zekkos A, Boutwell GP, Briaud JL, Cheung C, Cobos-Roa D, Ehrensing L, Govindasamy AV, Harder LF Jr, Inkabi KS, Nicks J, Pestana JM, Porter J, Rhee K, Riemer MF, Rogers JD, Storesund R, Vera-Grunauer X, Wartman J (2008a) New Orleans and Hurricane Katrina. I: introduction, overview, and the east flank. *J Geotech Geoenviron Eng* 134(5):701–717
- Seed RB, Bea RG, Athanasopoulos-Zekkos A, Boutwell GP, Bray JD, Cheung C, Cobos-Roa D, Cohen-Waerber J, Collins BD, Harder LF Jr, Kayen RE, Pestana JM, Riemer MF, Rogers JD, Storesund R, Vera-Grunauer X, Wartman J (2008b) New Orleans and Hurricane Katrina. IV: Orleans East Bank (Metro) Protected Basin. *J Geotech Geoenviron Eng* 134(5):762–779
- Serre D, Peyras L, Tourment R, Diab Y (2008) Levee performance assessment methods integrated in a GIS to support planning maintenance actions. *J Infrastruct Syst* 14(3):201–213
- Sills GL, Vroman ND, Wahl RE, Schwanz NT (2008) Overview of New Orleans levee failures: lessons learned and their impact on national levee design and assessment. *J Geotech Geoenviron Eng* 134(5):556–565
- Song CR, Kim J, Wang G, Cheng AHD (2011) Reducing erosion of earthen levees using engineered flood wall surface. *J Geotech Geoenviron Eng* 137(10):874–881

- Storesund R, Bea RG, Huang Y (2010) Simulated wave-induced erosion of the Mississippi River–Gulf Outlet Levees during Hurricane Katrina. *J Waterw Port Coast Ocean Eng* 136(3):177–189
- Ubilla J, Abdoun T, Sasanakul I, Sharp M, Steedman S, Vanadit-Ellis W, Zimmie T (2008) New Orleans levee system performance during hurricane Katrina: London Avenue and Orleans canal south. *J Geotech Geoenviron Eng* 134(5):668–680
- Weng MC, Wu MH, Ning SK, Jou YW (2011) Evaluating triggering and causative factors of landslides in Lawnon River Basin, Taiwan. *Eng Geol* 123:72–82
- Wu CH, Chen SC, Chou HT (2011) Geomorphologic characteristics of catastrophic landslides during typhoon Morakot in the Kaoping Watershed, Taiwan. *Eng Geol* 123:13–21
- Xu Y, Li L, Amini F (2012) Slope stability analysis of earthen levee strengthened by high performance turf reinforcement mat under hurricane overtopping flow conditions. *Geotech Geol Eng* 30(4):893–905